

Contents lists available at ScienceDirect

Chemical Engineering Research and Design



journal homepage: www.elsevier.com/locate/cherd



Investigating the impact of surfactant-salt feed solution on PTFE membrane performance under varying feed and permeate temperatures in membrane distillation

Atefeh Tizchang ^{a,b}, Itzel Alcaraz Bernades ^{a,b}, Morgan Abily ^c, Hussam Jouhara ^{d,e}, Luca Montorsi ^{f,g}, Wolfgang Gernjak ^{a,h,*}

- ^a Catalan Institute for Water Research (ICRA), Girona 17003, Spain
- ^b University of Girona, Girona 17003, Spain
- ^c Université Côte d'Azur, Observatoire de la Côte d'Azur, CNRS, IRD, Géoazur, France
- d Heat Pipe and Thermal Management Research Group, College of Engineering, Design and Physical Sciences, Brunel University London, UB8 3PH, United Kingdom
- ^e Vytautas Magnus University, Studentu Str. 11, Akademija, Kaunas Distr., LT-53362, Lithuania
- f Department of Science and Methods for Engineering, University of Modena and Reggio Emilia, Reggio Emilia 42122, Italy
- g InterMech-MO.RE, University of Modena and Reggio Emilia, Modena 41121, Italy
- ^h Catalan Institution for Research and Advanced Studies (ICREA), Barcelona 08010, Spain

ARTICLE INFO

Keywords: Membrane wetting Thermal performance Surfactant Direct contact membrane distillation

ABSTRACT

Membrane distillation (MD) is a temperature-driven technology suitable for treating industrial wastewater, especially when utilizing low-grade heat sources like waste heat or renewable energy. Despite its potential, largescale application of MD faces challenges due to high energy demands and operational instability caused by membrane fouling and wetting, particularly when surfactants are present. This study evaluated the thermal performance of a lab-pilot MD system using two commercial PTFE membranes. Initial experiments used saline feed solutions at varying feed and permeate temperatures. Subsequent tests introduced a non-ionic surfactant (Triton X-100), with and without NaCl, to investigate membrane fouling and wetting behavior. Results showed that higher feed temperatures increased permeate flux across all conditions, but also accelerated fouling and wetting, thereby shortening operational time. Notably, in the absence of NaCl, membrane degradation occurred more slowly, resulting in more stable performance. The novelty of this study lies in revealing the combined effect of salinity and non-ionic surfactants on the fouling and wetting performance of commercially available PTFE membranes in membrane distillation. Using a comprehensive two-stage experimental approach, the work systematically correlates MD system performance with membrane degradation mechanisms under feed conditions representative of real industrial wastewater. This dual focus not only uncovers the interplay between surfactants and salts but also provides practically relevant insights into the reliability and applicability of PTFE membranes in industrial MD operations.

1. Introduction

As human activities including industrial processes continue to grow unsustainably, the adoption of novel technologies to treat industrial wastewater becomes crucial (Ramlow et al., 2019; Suárez et al., 2022). Membrane separation technology is a proper candidate for achieving this goal due to its low footprint and versatility (Yao et al., 2020a; Kalla, 2021). Conventional pressure driven membrane technologies can have drawbacks such as needing to overcome osmotic pressure for saline

wastewater, whereas membrane distillation (MD) technologies operate at much lower hydraulic pressures, and this makes it a desirable choice for treating challenging, saline wastewater (Powdered activated carbon PAC – vacuum-assisted air gap membrane distillation V-AGMD hybrid system to treat wastewater containing surfactants: Effect of operating conditions,; Yadav et al., 2021; Leaper et al., 2021).

The MD process is a versatile separation process based on the partial pressure difference of water vapor across a hydrophobic membrane (Chew et al., 2017a; Ali et al., 2024). The MD principle can be applied in

^{*} Corresponding author at: Catalan Institute for Water Research (ICRA), Girona 17003, Spain. E-mail address: wgernjak@icra.cat (W. Gernjak).

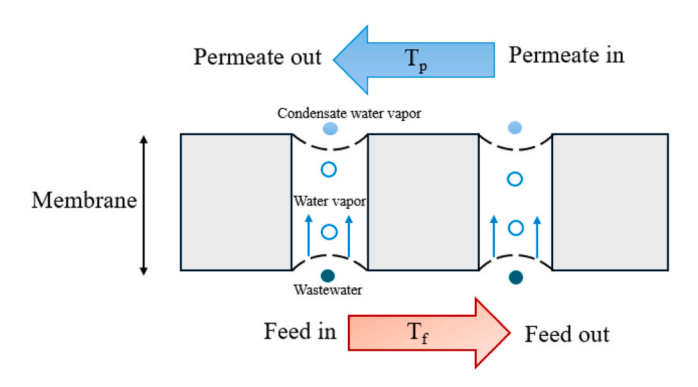


Fig. 1. General schematic of the DCMD process.

several different engineered configurations, which have been extensively reviewed by Francis et al (Francis et al., 2022). One of the most common configurations for MD systems is DCMD (direct contact membrane distillation). In this process a feed flow with a higher temperature is in contact with the permeate flow with a lower temperature through the membrane as a physical barrier (García et al., 2018; Bahmanyar et al., 2012). Due to the higher temperature of the feed solution, water evaporates and diffuses through the membrane pores and gets condensed on the permeate side of the membrane with lower temperature (Alkhudhiri et al., 2012; Khayet, 2011; Pangarkar et al., 2016). The schematic of this process is represented in Fig. 1.

MD systems can usually be coupled with low-quality heat sources such as solar or waste heat which can be considered as the major advantage of using them (Ullah et al., 2018; Deshmukh et al., 2018; Afsari et al., 2022). However, MD has a limited implementation, mainly due to its higher energy demands compared to pressure-driven processes (Criscuoli and Carnevale, 2022; Rezaei et al., 2018). Additionally, it has lower thermal efficiency than multi-stage flash processes, hindering its industrial adoption (Zhang et al., 2015). Therefore, an analysis of MD's energy efficiency, particularly in DCMD, can help identify its strengths and weaknesses to pave the way for development of this technology for large-scale and small-scale portable uses (Ullah et al., 2018).

Fouling and wetting of the membrane are still major challenges that are faced using these systems at large scale for a prolonged period of operation (Choudhury et al., 2019; Tijing et al., 2015). Membrane fouling occurs from the build-up of unwanted substances on the membrane surface and within its pores which will cause permeate flux to decline. Excessive membrane fouling can lead to membrane wetting such as surfactant-induced wetting. Once wetting happens, the feed solution will pass through the membrane pores, degrading the permeate quality (Chang et al., 2022). Feed composition that is highly dependent on different industries has the greatest impact on the wetting phenomenon (Lu et al., 2019). One of the components that are present in the production process of many products such as paints, cosmetics, pesticides, plastics etc. are surfactants (Chew et al., 2019). In membrane technology, feed solutions containing surfactants will create a surfactant deposition on the membrane surface and can wet the hydrophobic membrane by decreasing both the membrane surface contact angle and feed surface tension which will severely compromise its separation efficiency (Yao et al., 2020b; Tomczak and Gryta, 2021; Guo et al., 2023).

Several studies have been done to tackle the wetting and fouling problem caused by the presence of surfactants in the feed solutions. Chew et al. studied the wetting behavior of a Polyvinylidene fluoride (PVDF) membrane using four different types of surfactants individually (Chew et al., 2017b). The results showed that hydrophilic-lipophilic balance (HLB) and critical micelle concentration (CMC) are two main factors of surfactants that have direct impact on the membrane wetting phenomenon. Surfactants with lower HLB values are more hydrophobic, resulting in stronger hydrophobic interactions. These interactions are dictated by the HLB value of the surfactant (Chew et al., 2019). A higher

HLB value indicates a more hydrophilic surfactant, which exhibits a higher affinity for the aqueous feed. When the surfactant concentration surpasses the CMC value, surfactant monomers aggregate more densely on the membrane surface from the hydrophobic head groups due to hydrophobic interactions, potentially causing membrane fouling. Once attached to the membrane surface, surfactants with larger hydrophilic head groups are more likely to attract the aqueous feed toward the membrane, leading to pore wetting (Chew et al., 2017b; Eykens et al., 2017). Therefore, to compare the membrane behavior in the case of wetting, surfactant characteristics such as HLB play a key role (Chew et al., 2017b).

Although the use of composite membranes for MD processes in bench-scale laboratory tests has been quite effective regarding the reduction of fouling in membranes, they are not yet suitable for commercial production due to the absence of large-scale fabrication methods (Feng et al., 2023). Therefore, Feng et al., investigated the impact of pretreating MD hydrophobic membranes using a surfactant solution in the feed under controlled conditions to improve the fouling resistance of the membrane. They showed that by pretreating the MD membranes with surfactants a hydration layer forms on the surface of the membrane which protects membranes from fouling (Feng et al., 2023).

Another study investigating the impact of adding diverse types of surfactants on DCMD performance revealed that the use of nonionic surfactants caused the greatest decline in permeate flux. The rate of decline increased with higher surfactant concentrations and feed temperatures but decreased with higher salt concentrations in the feed stream. This implies that feed temperature and salt concentration are crucial variables when examining the permeate flux in the presence of surfactants (Wen et al., 2018). Lou et al. studied the influence of varied cations on membrane wetting and they showed that the surfactant-induced membrane wetting was closely linked with the presence of coexisting cations. Based on the results obtained from this study, the addition of K^+ and Ca^{2+} notably accelerated membrane wetting compared to Na^+ , Mg^{2+} and Al^{3+} . Also, the combination of Ca^{2+} and low feed temperature successfully relieved the membrane wetting (Lou et al., 2022).

In this study, we did a comprehensive investigation to scrutinize the behavior of the commercial Polytetrafluoroethylene (PTFE) membranes in DCMD systems in terms of thermal analysis evaluation and the membrane's fouling/wetting behavior. At first, regarding the thermal analysis evaluation, a saline feed solution was prepared and the thermal behavior of the MD system in a range of different feed and permeate temperatures was studied using parameters such as specific energy consumption (SEC) and gained output ratio (GOR). Then, in the second phase of experiments, feed solutions containing three different concentrations of Triton X-100, a non-ionic surfactant, were prepared to investigate the fouling/wetting behavior of PTFE commercial membranes in the MD process as a function of inlet feed and permeate temperatures. Although testing additional surfactant types (anionic and cationic) could further broaden the scope of the findings, only Triton X-100 was tested to reduce complexity and enable a systematic investigation of the coupled effects of salinity and surfactants on PTFE membranes. Finally, to simulate realistic industrial wastewater conditions, a saline feed solution containing the surfactant was used to evaluate membrane performance and examine the impact of the combined presence of salinity and surfactants. Later, to confirm the wetting and fouling characteristics in the membranes, morphological analyses such as scanning electron microscopy (SEM) equipped with energy-dispersive X-ray spectroscopy (EDX) were conducted. The objectives of this study were: (1) to assess the thermal performance of the MD system with a saline feed solution under varying feed and permeate temperatures; (2) to examine membrane flux performance using a feed solution containing surfactants at different feed and permeate temperatures, and (3) to explore the co-existing impacts of NaCl with surfactants in the feed solution on the membrane performance.

Table 1Characteristics of the membranes used in the MD experiments.

Item	M-P	M-T
Membrane material	PTFE	PTFE
Support layer	PP	PET
Average pore size (µm)	0.2	0.22
Average thickness (µm)	200	150
Air permeability at 0.13kPa (L m ⁻² s ⁻¹)	3–5	3–5
Contact angle (deg)	136 ± 4	130 ± 4
Liquid entry pressure or water LEPw (kPa)	> 350	> 300
Max-continuous operating temperature (°C)	80 ± 1	80 ± 1

2. Materials and methods

2.1. Membranes and chemicals

The membranes used for the MD experiments, M-T and M-P, were both PTFE membranes with PET and PP support layer purchased from Memsift Innovation Pte Ltd. The characteristics of each membrane are presented in Table 1.

Sodium chloride (NaCl, 99.4 %) was used for preparing saline feed solutions and Triton X-100 as a nonionic surfactant was purchased from Sigma-Aldrich for preparing feed solutions containing surfactant. The properties of the surfactant used in this study are presented in Table 2.

2.2. Lab-pilot DCMD experiment

MD experimental procedures were performed using the lab-pilot membrane distillation system purchased from Memsift Innovation Pte Ltd that can function in four different configurations, DCMD, vacuum MD (VMD), air gap MD (AGMD) and sweeping gas MD (SGMD). In this study only the DCMD configuration has been used. The overall schematic flowchart of the system is shown in Fig. 2.

The lab-pilot setup consisted of three main tanks, a feed tank, a permeate tank and a product tank shown in Fig. 3(a). The feed tank and permeate tanks were connected to the heat exchanger HE-1 and a chiller respectively (Fig. 3(a)(b)). Heat exchangers and the chiller could be controlled automatically and, with the electronic control panel placed on the front side of the unit, the temperatures of the feed and permeate solutions adjusted. The MD unit had two pressure gauges, two flow meters, two conductivity meters and eight temperature sensors. Feed and permeate conductivity and flow on these streams were constantly monitored using two small screens on the front side of the unit.

The membrane module shown in Fig. 3(b) is a flat sheet membrane module consisting of two different channels each with a height of 5 mm. The module was divided by an active membrane area of $450~\text{cm}^2$ and was cut into $30^*15~\text{cm}^2$ dimensions to fit the designated area of the membrane module. For each experiment a new membrane was used. The feed and permeate streams were in counter-current mode for all the experiments to better maintain the temperature difference between

Table 2
Surfactant used in this study (Merck et al.).

Surfactant (molecular weight)	Туре	CMC (mM)	HLB	Chemical structure
Triton X-100 (626 g/mol)	Nonionic	0.22-0.24	13.5	H ₃ C H ₃ C CH ₃

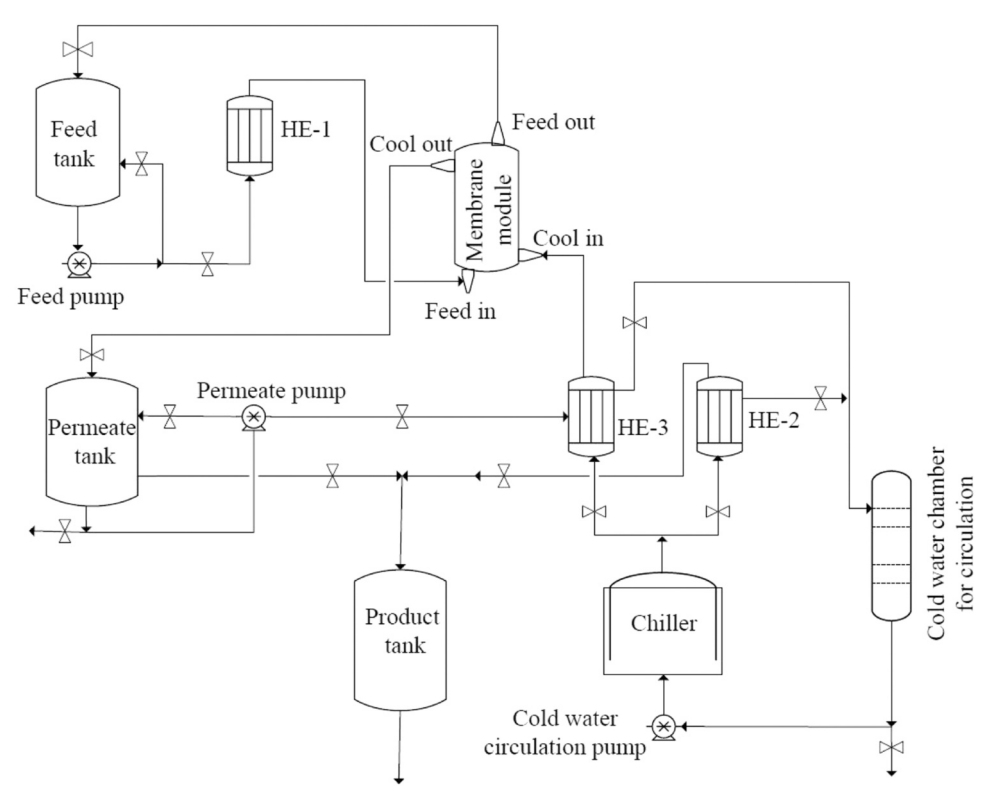


Fig. 2. The schematic diagram of the lab-pilot scale MD system.

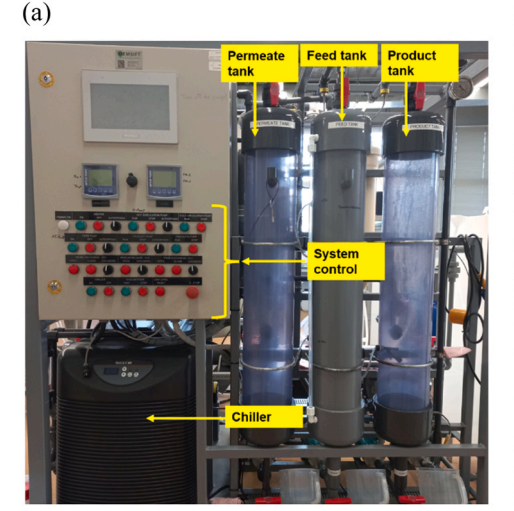






Fig. 3. (a) Front side of the MD unit, (b) Back side of the MD unit.

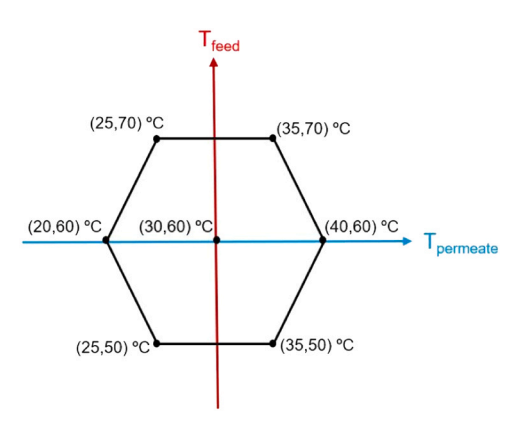


Fig. 4. The selected inlet feed and permeate temperatures for all the experiments in this study.

them. The flow rates of feed and permeate sides were set to 5 ${\rm L}\ {\rm min}^{-1}$ for all the experiments.

2.3. Experimental procedure

To determine the inlet feed and permeate temperatures for assessing the membrane flux and thermal performance, a temperature range of 50 °C to 70 °C for the feed, and 20 °C to 40 °C for the permeate were deemed suitable, and final experimental temperatures were selected resembling closely a uniform shell experimental design (Fig. 4). Thus, experiments were performed with three different inlet feed temperatures of 50, 60 and 70 °C, and five different inlet permeate temperatures of 20, 25, 30, 35 and 40 °C.

For each experiment 13 liters of 3 wt% NaCl feed solution was prepared, and membrane flux, salt rejection and thermal performance indicators were measured during 7 h of experiment. The addition of 1 wt% NaCl solution will reduce the CMC value of Triton X-100 by approximately 50 % (Akhlaghi and Riahi, 2019). By increasing the salinity, the CMC value will decrease correspondingly. On the other hand, the CMC of the nonionic surfactants decreases with increasing temperature and then slowly increases at higher temperatures (Shadloo et al., 2022). Therefore, there are two factors impacting the characteristics of feed simultaneously during the experiments as the separation process continues. The initial concentration of NaCl in the feed solution was considered 3 wt% to avoid further complications since the principal variant in this study was inlet feed and permeate temperature.

For the next series of experiments the impact of adding different concentrations of surfactants to the feed solution at different inlet feed temperatures was studied. Thus, for each test 13 liters of feed solution containing 25, 50 and 75 mg L $^{-1}$ (< CMC value) surfactant was prepared to study the fouling and wetting phenomena in each membrane. Each experiment was performed in the presence and absence of salt to study the impact of salt in the feed solution on membrane flux performance. For these experiments three different temperatures of 25 and 70 °C, 30 and 60 °C and 25 and 50 °C were selected for the permeate and feed temperatures, respectively. It should be noted that experiments were conducted without replicates; nevertheless, the results showed consistent trends, supporting the reliability of the conclusions.

To investigate the morphologies and elemental compositions of pristine and used membranes, Field Emission Scanning Electron Microscopy (FE-SEM) coupled with Energy-Dispersive X-ray spectroscopy (EDX), was used to check the presence of surfactants and NaCl on the surface of the membranes used. For preparation of the samples for analyzing the surface morphologies, first all the samples were cleaned by water and then they were mounted on a stub with a carbon adhesive tape and coated with an evaporator coater (EMITECH K950 turbo, Germany), and then examined by FE-SEM (TESCAN Clara 2. Czech Republic). Also, for the preparation procedure of the samples for crosssection SEM imaging, the samples were cut and embedded in crosssection in epoxy resin AXSON RSF816. Then, they were metallographically polished using abrasive paper (P80, P150, P240, P400, P800, P1200, and P2000), followed by a final polish using synthetic cloths and alumina of 9.5, 3, and 1 micron. They were mounted on stubs and coated with carbon (EMITECH K950 turbo evaporator, Germany). Finally, they were examined by scanning electron microscope.

2.4. Performance parameters evaluated in this study

The treated water from the membrane process was collected as an overflow of the permeate tank in the product tank and is called permeate flux. The permeate flux was calculated using Eq. (1):

$$J = \frac{V}{A\Delta t} \tag{1}$$

where J is the permeate flux (L m⁻² h⁻¹), V is the volume of the treated water collected from the product tank (L), A is the effective membrane area (m²), which was 0.045 m², and Δt was the time difference (h).

The membrane rejection rate (R) was calculated using Eq. (2):

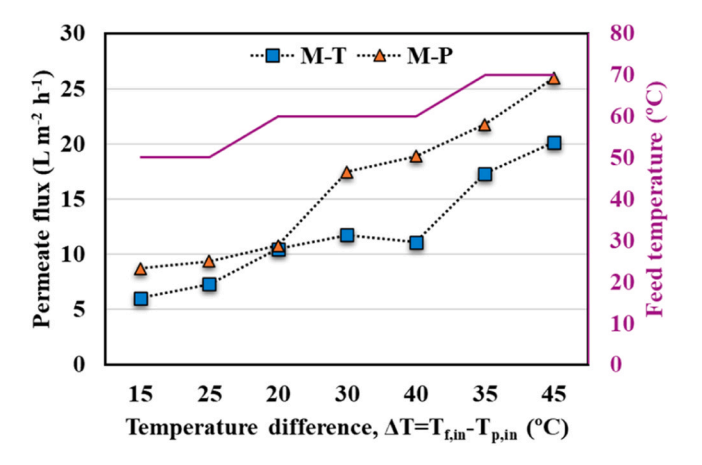


Fig. 5. Permeate flux as a function of feed and permeate temperature.

$$R \quad \% = \frac{Cf - Cp}{Cf} \quad \times 100 \tag{2}$$

where C_f in the initial conductivity ($\mu S \text{ cm}^{-1}$) of the feed and C_p is the conductivity of the permeate.

GOR is a fundamental performance indicator that is defined as the ratio of the required energy for feed evaporation to the total energy input to the system, and is expressed in the following Eq. (3) (Criscuoli and Carnevale, 2022):

$$GOR = \frac{JA\Delta H}{E_{in}} \tag{3}$$

where J is the permeate flux (kg m $^{-2}$ h $^{-1}$), ΔH is the enthalpy of vaporization of water (kJ kg $^{-1}$) and E_{in} is the total thermal energy supplied to the system (kW).

The specific energy consumption (SEC) is a principal factor for evaluating the thermal performance of MD system, and it describes the total thermal energy supplied to the system to produce a unit mass of the product that can be calculated as below (Elmarghany et al., 2019):

$$SEC\left(\frac{kWh}{m^3}\right) = \left(\frac{Q\rho}{JA}\right) / 3600 \tag{4}$$

where ρ is the water density (kg m⁻³), and Q is the total heat flux through the membrane (kW), calculated by using Eq. (5).

$$Q = m_f \quad C_P \quad (\quad T_{f,in} - T_{f,out})$$
 (5)

where m_f is the feed mass flow rate (kg s $^{-1}$), C_p in this equation is the feed water specific heat capacity (kJ kg $^{-1}$ °C $^{-1}$), $T_{f,in}$ and $T_{f,out}$ are the inlet and outlet feed water temperatures, respectively (°C).

3. Results and discussion

3.1. Membrane flux and thermal performance during DCMD process

To study the impact of inlet feed and permeate temperature on the permeate flux, a set of MD experiments was conducted to measure the permeate flux at different feed and permeate temperatures for both M-T and M-P membranes. All the MD experiments were conducted using feed solutions containing 3 % NaCl, lasting for 7 h, with the feed and permeate flow rate maintained at 5 L min⁻¹. The results of this experiment are shown in Fig. 5. In all cases, by increasing the inlet feed temperature the permeate flux increased. For instance, for the M-T membrane the permeate flux was 6.03 and 7.30 L m⁻² h⁻¹ when the inlet feed temperature was 50 °C and the permeate temperature was 35 and 25 °C, respectively. However, when the inlet feed temperature rose to 70 °C, the permeate flux tripled to 17.33 and 20.15 L m⁻² h⁻¹ for permeate temperatures of 35 and 25 °C, respectively. So not only does the higher inlet feed temperature increase the permeate flux, but also the greater difference between feed and permeate temperatures leads to a higher permeate flux. The same behavior was observed for the M-P membrane. The permeate flux rose from $8.73 \,\mathrm{L m^{-2} \,h^{-1}}$ to $21.75 \,\mathrm{L m^{-2}}$ h⁻¹ for inlet feed temperatures of 50 °C and 70 °C, respectively.

The overall system energy efficiency is measured as GOR using Eq. 3, and the results are presented in Fig. 6(a). In general, a higher GOR value signifies reduced thermal energy consumption for each unit of distillate produced. Although capital costs can be substantial (Swaminathan et al., 2016a), thermal energy accounts for the largest portion of water production costs in MD systems. Therefore, MD companies have concentrated on applications leveraging waste heat energy available from power plants and other sources (Swaminathan et al., 2016b). GOR, which is proportional to MD thermal efficiency, together with membrane flux are usually used to assess the performance of MD systems (Swaminathan et al., 2018). As shown in Fig. 6(a), GOR increased for both M-T and M-P membranes by increasing the inlet feed temperature. Moreover, for each inlet feed temperature, by increasing the difference between feed and permeate temperatures, GOR was escalated. With limited heat loss to the environment, increasing the feed temperature can enhance GOR as well as thermal efficiency.

The effects of different feed and permeate temperatures on specific energy consumption (SEC) were calculated using Eq. 4 and the results are presented in Fig. 6(b). Detailed data about average feed inlet and outlet temperatures used to calculate SEC for each experiment are presented in Tables S1 and S2. As indicated, increasing the inlet feed temperature led to a reduction in SEC for both M-T and M-P membranes. For the M-T membrane the SEC dropped from 3302 kWh m $^{-3}$ for the lowest feed temperature (50 °C) and smallest temperature difference of 15 °C between feed and permeate, to 1887 kWh m $^{-3}$ for the highest feed temperature of 70 °C and highest temperature difference of 45 °C between feed and permeate. The same behavior was observed by the M-P

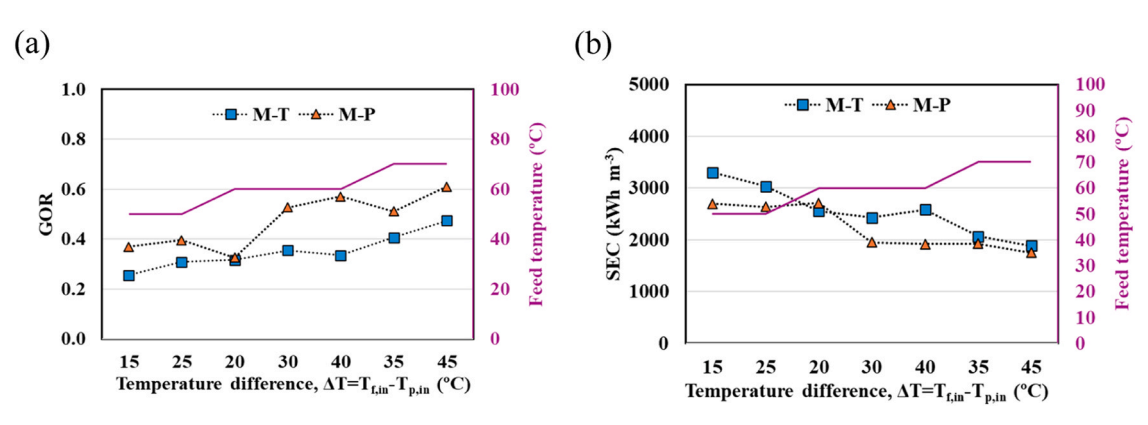


Fig. 6. GOR and SEC values as a function of feed and permeate temperatures.

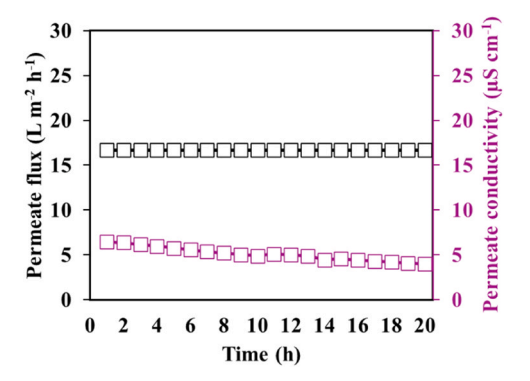


Fig. 7. Integrity test for M-T membrane with 3 wt% NaCl feed solution (feed and permeate temperatures of 70 and 25 °C respectively).

membrane and the SEC value decreased from 2697 kWh m $^{-3}$ to 1751 kWh m $^{-3}$ for the lowest feed temperature of 50 °C and smallest temperature difference of 15 °C between feed and permeate, and the highest feed temperature of 70 °C and greatest temperature difference of 45 °C between feed and permeate, respectively. The results show that increasing the feed temperature and maintaining the highest temperature difference between feed and permeate can lead to a reduction of total energy consumption of about 35 % which can be cost effective. It is

important to note that all these SEC values apply to a single-stage operation; employing a multi-stage system can significantly enhance thermal performance efficiency. In fact, MD processes reported in the literature exhibit significantly higher energy consumption than other separation technologies. In terms of energy requirements, reverse osmosis (RO) typically consumes 1–7 kWh m⁻³, multi-stage flash (MSF) distillation 70–84 kWh m⁻³, multi-effect distillation (MED) 42–67 kWh m⁻³, and mechanical vapor compression (MVC) 6.5–12 kWh m⁻³. In comparison, the energy consumption of MD is considerably higher than these conventional desalination methods. Therefore, it is crucial for MD to target both high water flux and efficient heat recovery (Miladi et al., 2019).

Permeate flux and thermal characteristics of the M-T and M-P membranes are summarized in Tables S3 and S4.

3.2. The fouling/wetting behavior of membranes during DCMD process

To assess the integrity of the M-T membrane, an initial test was carried out using 3 wt% NaCl aqueous feed solution for 20 h with feed and permeate temperatures of 70 and 25 °C, respectively. As illustrated in Fig. 7 during 20 h of experiment the permeate flux of M-T membrane stabilized at around $16.5~L~m^{-2}~h^{-1},$ with the conductivity decreasing slightly from $6.5~to~4~\mu\text{S}~cm^{-1},$ showing that no wetting was observed in the M-T membrane when only NaCl solution was used as feed solution,

-□- Permeate flux (L m⁻² h⁻¹) -□- Permeate conductivity (μS cm⁻¹)

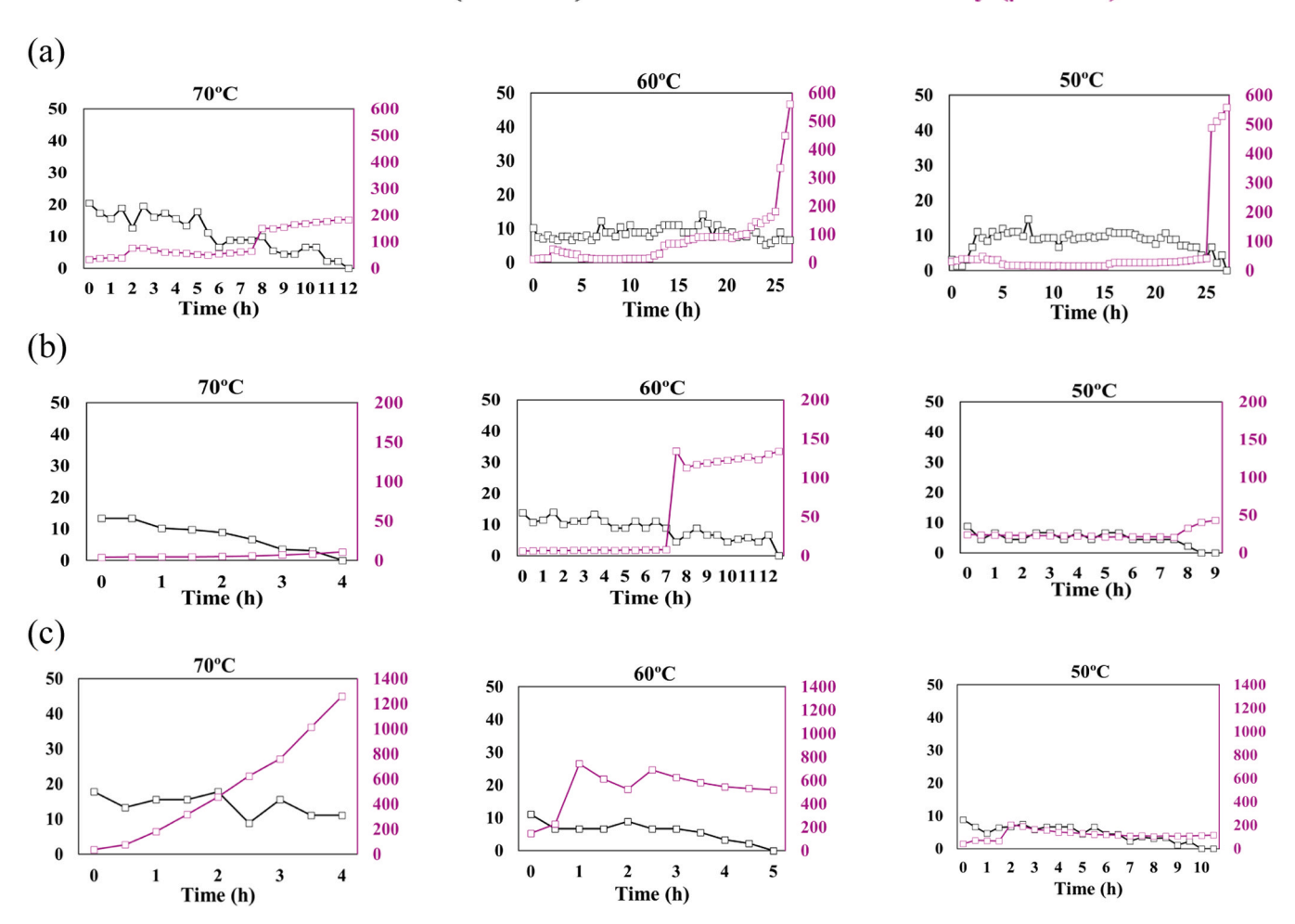


Fig. 8. The effect of inlet feed and permeate temperatures on the DCMD performance using M-T membrane with feed solution containing 3 wt% NaCl and (a) 25 mg L^{-1} surfactant, (b) 50 mg L^{-1} surfactant, (c) 75 mg L^{-1} surfactant at feed temperatures at 70, 60 and 50 °C and permeate temperatures at 25, 30 and 25 °C respectively.

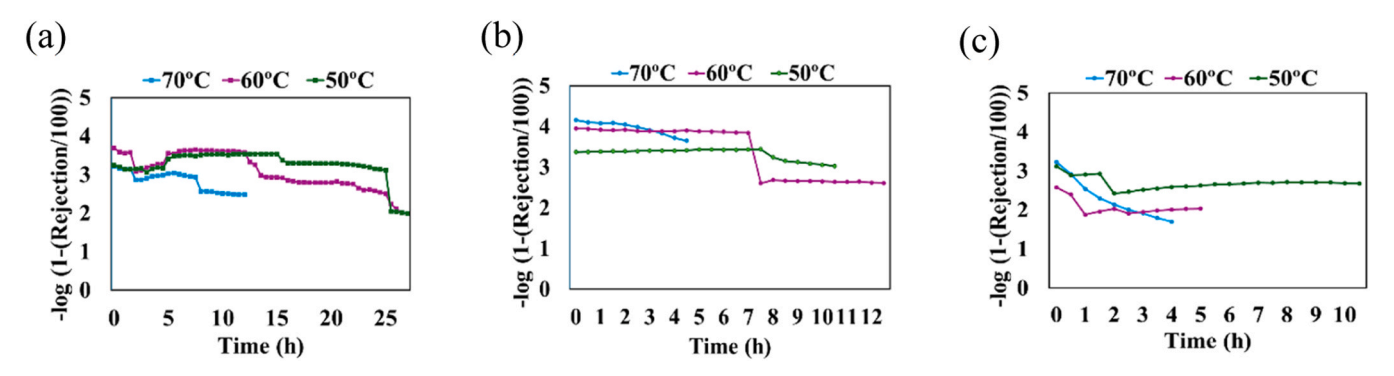


Fig. 9. The effect of inlet feed temperature on M-T membrane's rejection with feed solution containing 3 wt% NaCl and (a) 25 mg L^{-1} surfactant, (b) 50 mg L^{-1} surfactant, (c) 75 mg L^{-1} surfactant.

and the salt rejection was maintained > 99.99 % throughout the whole process.

Fig. 8 represents the effect of inlet feed temperature on the DCMD performance using the M-T membrane with a feed solution containing 3 wt% NaCl and three different concentrations of surfactant. As demonstrated, an increase in feed temperature from 50 $^{\circ}$ C to 70 $^{\circ}$ C

almost for all the cases resulted in a higher initial flux which is due to the higher water partial pressure and lower viscosity of the solution in the feed (Elcik et al., 2020). However, the higher the feed temperature, the sharper the decline in permeate flux which results in a shorter overall period of operation (Wen et al., 2018). With a 75 mg L $^{-1}$ concentration of surfactant and a feed temperature of 50 °C, the DCMD performance

-□- Permeate flux (L m⁻² h⁻¹) -□- Permeate conductivity (μS cm⁻¹)

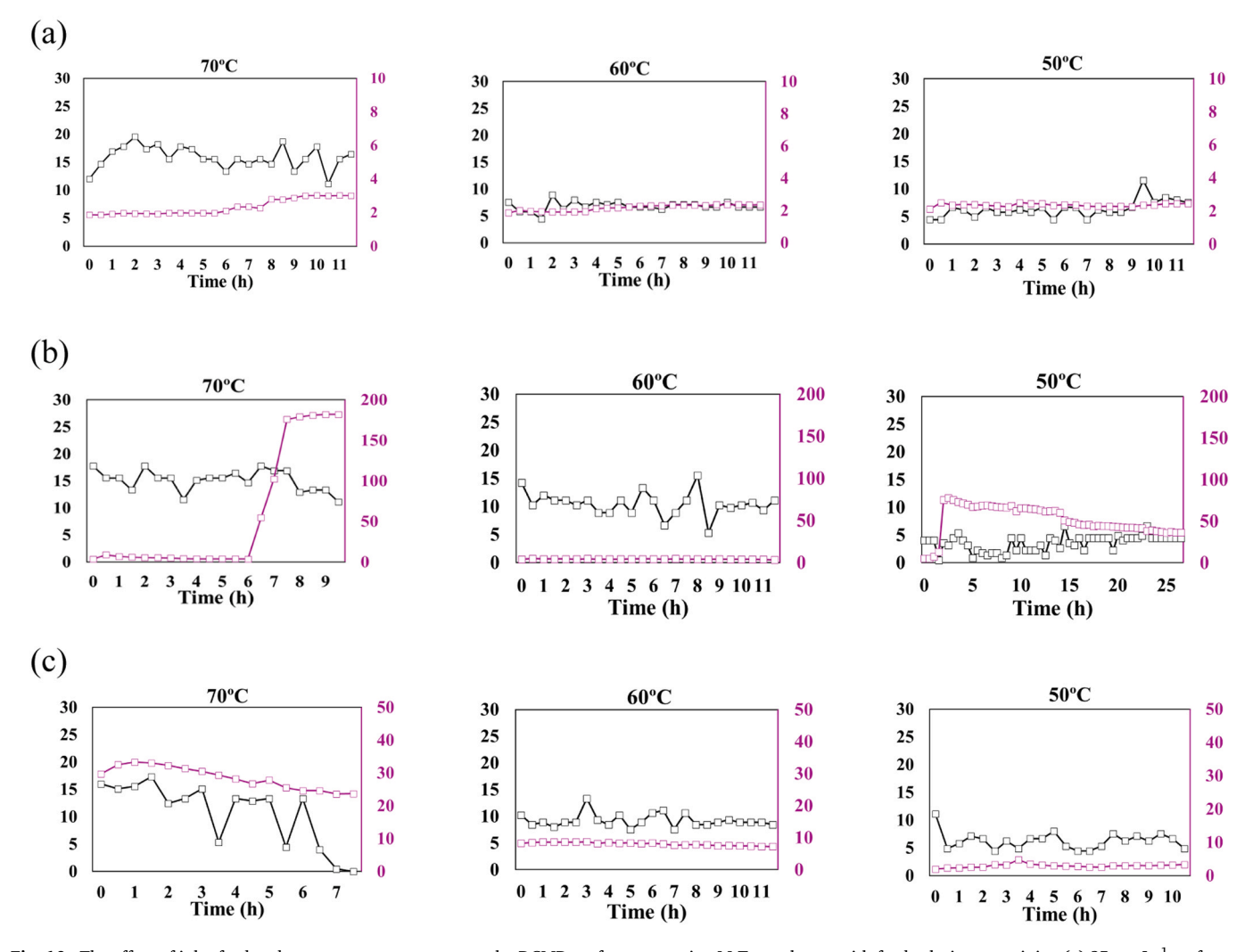


Fig. 10. The effect of inlet feed and permeate temperatures on the DCMD performance using M-T membrane with feed solution containing (a) 25 mg L⁻¹ surfactant (b) 50 mg L⁻¹ surfactant (c) 75 mg L⁻¹ surfactant at feed temperatures at 70, 60 and 50 °C and permeate temperatures at 25, 30 and 25 °C respectively.

-□- Permeate flux (L m⁻² h⁻¹) -□- Permeate conductivity (μS cm⁻¹)

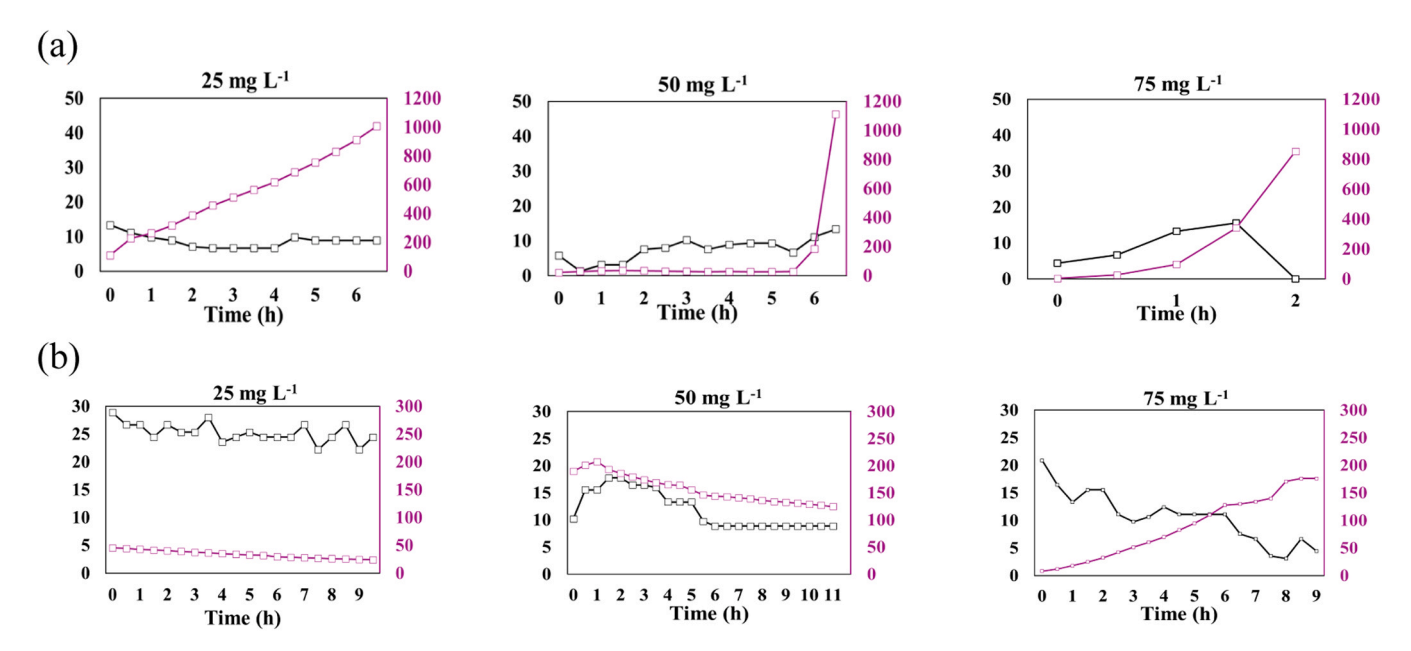


Fig. 11. The effect of the different concentrations of surfactants on the DCMD performance using M-P membrane with feed and permeate temperature of 60 and 30 °C respectively with 3 wt% NaCl (a), and without NaCl (b).

regarding the permeate flux was quite stable, and no drastic change was noticed for permeate conductivity. In this case the whole operation lasted for ten hours until the flux dropped to zero which showed potential fouling in the membrane. By increasing the feed temperature to 60 °C, the permeate flux dropped to zero after only five hours of experiment, which was due to the fouling in the membrane. Also, in this case an increase in permeate conductivity was observed which can represent the potential wetting phenomenon in the membrane, but since the contaminant rejection was mostly maintained at more than 99 % during the whole operation (shown in Fig. 9(c)), the impact of potential wetting on the membrane can be deemed negligible. Changing the feed inlet temperature to 70 °C caused a sudden increase in the permeate conductivity and a decline in rejection from 99.9 % to 98 % in the early hours of experiments which indicates the wetting phenomenon had already happened in the membrane.

By decreasing the concentration of the surfactant from 75 mg L^{-1} to 50 mg L^{-1} when the feed temperature was 50 °C, the membrane was completely fouled after almost nine hours of experiment. When the inlet feed temperature increased from 50 °C to 60 °C, the operation continued for more than twelve hours, and a sharp increase in conductivity was observed, so there might have been some wetting in the membrane, however, the overall rejection was maintained at more than 99 %. When the inlet feed temperature was 70 °C, the same operation could only last four hours before complete fouling happened.

When the concentration of surfactant in the feed solution was reduced to $25 \, \mathrm{mg \, L^{-1}}$, with the inlet feed temperature at 70 °C, the operations stopped due to the potential fouling in the membrane after around eleven hours of experiment. But when the inlet feed temperature decreased to 60 °C and 50 °C the separation process continued for more than twenty-five hours with an almost constant amount of permeate flux, however, in the final hours of the experiment a great rise in the permeate conductivity was observed which caused the salt rejection to drop from 99.98 % to 99 % (Fig. 9(a)). This increase in the permeate conductivity can be attributed to the potential wetting phenomenon in some parts of the membrane. It is worth noting that all the changes in the rejection values shown in Fig. 9 are represented on a log-scale basis for better visualization of data.

The same experiments were done without salt in the feed solution, and the results are shown in Fig. 10. With a 75 mg L^{-1} concentration of surfactant and feed temperature of 50 °C, the permeate flux was stable for more than 10 h and a low conductivity of less than 5 µS cm⁻¹ was maintained during the process. The same behavior was seen when the inlet temperature was increased to 60 °C with the stable conductivity around 5 µS cm⁻¹ and permeate flux of 10 L m⁻² h⁻¹. However, by increasing the feed temperature to 70 °C, the permeate conductivity increased more than 3 times, and in the case of permeate flux, after some fluctuations, it dropped to zero after 7 h of operation which shows complete fouling. With the same feed temperature (70 °C) and decreasing the surfactant concentration to 50 and 25 mg ${\it L}^{-1}$, the overall operation time before complete fouling or wetting increased to more than 9 and 11 h, respectively. To elaborate, when the surfactant concentration was 50 mg L⁻¹ after 6 h of operation the permeate conductivity had a drastic rise from 3 to 50 μS cm⁻¹ and then 100 μS cm⁻¹ which signified the potential wetting in some parts of the membrane, but the operation continued to more than 9 h without complete fouling. With the lower concentration of surfactant (25 mg L^{-1}), the operation continued for more than 11 h without witnessing any drastic change in permeate conductivity.

Based on all the results presented in Figs. 8 and 10, the DCMD system performed more stably regarding permeate flux and conductivity in the absence of NaCl in the feed solution, and it can be seen especially by increasing the feed temperature. At 70 °C when the surfactant concentration was 50 and 75 mg L⁻¹, the operation lasted only 4 h with NaCl in the feed solution, however, without NaCl it continued for more than 7 h without complete fouling. It can be concluded that a feed solution solely containing surfactant does not lead to severe wetting. But the introduction of NaCl to the feed solution disrupted the stable wetting condition, leading to an unexpected shift in wetting behavior, which is due to the coexisting impact of salt by lowering the CMC and accelerating the wetting (Lou et al., 2022; Tan et al., 2019). In other words, the presence of NaCl in the solution lowers the repulsive action between the charged head groups of the surfactant molecules which will facilitate micellization at lower concentrations of surfactant (Miyagishi et al., 2001). As a result, the generated micelles can accumulate on the membrane surface

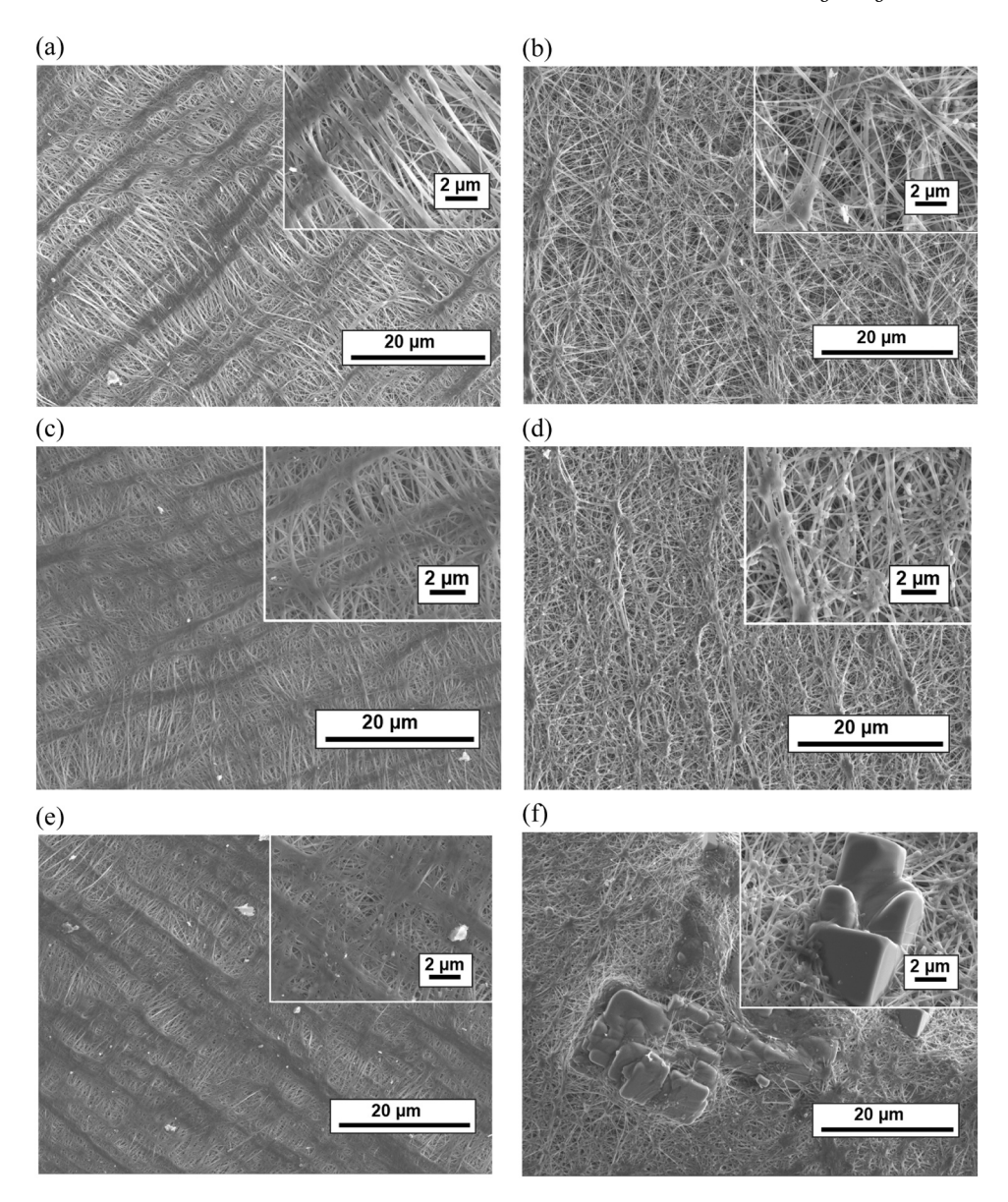


Fig. 12. Membrane surface morphology before and after DCMD process. (a) Pristine M-P, (b) Pristine M-P, (c) Used M-T membrane exposed to a feed solution containing 50 mg L^{-1} surfactant, (d) Used M-P membrane exposed to a feed solution containing 50 mg L^{-1} surfactant (e) Used M-T membrane exposed to a feed solution containing 50 mg L^{-1} surfactant and 3 % NaCl, (f) Used M-P membrane exposed to a feed solution containing 50 mg L^{-1} surfactant and 3 % NaCl, (feed and permeate temperatures of 60 and 30 °C respectively for all cases).

through interactions of their hydrophobic tails, while their hydrophilic head groups attract water from the feed side, thereby promoting pore wetting.

Fig. 11 shows the impact of adding different concentrations of surfactant to the feed solution at feed and permeate temperatures of 60 and 30 °C respectively with and without NaCl for the M-P membrane. In all the experiments performed with NaCl, wetting occurred sooner in comparison to the experiments without NaCl. When the feed surfactant concentration was 25 mg L^{-1} with NaCl, the increasing trend of permeate conductivity initiated immediately after starting the MD process and it reached almost 1000 μS cm $^{-1}$ after 6 h of operation. However, without NaCl in the feed solution for the same concentration of surfactant, the permeate conductivity was almost stable throughout the operation with the permeate flux being around 25 L m $^{-2}$ h $^{-1}$. By increasing the surfactant concentration to 75 mg L^{-1} with NaCl, the MD process was halted due to the complete fouling and potentially the wetting of the membrane, since not only the permeate flux dropped to zero, but also the permeate conductivity rose dramatically up to almost

900 μ S cm $^{-1}$. Without NaCl for the same surfactant concentration, the fouling and wetting phenomena were happening gradually after 9 h of experimentation. The results show the deteriorating impact of salinity in terms of membrane fouling and wetting in the presence of surfactants in the MD systems. The same results were observed for the M-T membrane.

By evaluating thermal parameters of the membrane and combining them with the permeate flux analyses, it can be concluded that from an operational perspective, optimum conditions for industrial application are not necessarily those that maximize a single parameter but rather those that balance high flux with acceptable SEC and sufficient GOR. For example, operating within a moderate feed temperature range (e.g., 55–60 °C in this study) and maintaining a 20–30 °C feed–permeate temperature difference appears to provide a practical compromise, yielding both reasonable flux and improved thermal efficiency without excessive energy penalties. This integrated view can serve as a more direct basis for selecting operating parameters and guiding design optimization of industrial MD systems.

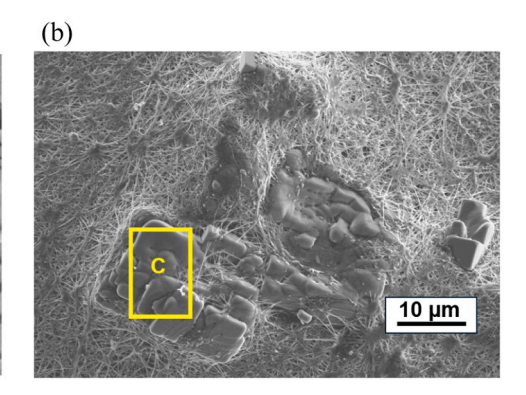


Fig. 13. Membrane surface morphology after DCMD process. (a) Used M-T membrane exposed to a feed solution containing 50 mg L⁻¹ surfactant and 3 % NaCl, (b) Used M-P membrane exposed to a feed solution containing 50 mg L⁻¹ surfactant and 3 % NaCl. (feed and permeate temperatures of 60 and 30 °C respectively for both cases).

Table 3Concentration (wt%) of elements on the membrane surface.

Area	С	0	F	Na	Cl	Si
a	50.51	0.74	35.99	11.20	0.96	0.59
b	54.49	-	45.06	0.21	-	0.24
c	42.09	0.68	1.62	24.00	31.61	-

3.3. EDX mapping and SEM imaging

Surface morphologies of the pristine and used M-T and M-P membranes are shown in Fig. 12. For both used membranes the inlet feed and permeate temperatures were fixed at 60 and 30 °C respectively, and the concentration of the surfactant was 50 mg L⁻¹. It can be seen in Fig. 12 that both pristine membranes have a uniform distinct porous surface, while in the presence of surfactant in the feed solution the surface morphology of the membranes seems denser compared to the pristine ones. Surfactant adsorption on hydrophobic surfaces is described as non-cooperative in the literature, meaning micelles are not created, and since Triton X-100 is a non-ionic surfactant, the adsorption is mostly based on hydrophobic interactions. Hence, single surfactant molecules form a monolayer on the surface of the membrane (Kronberg et al., 2014). For this reason, surface morphologies of the membrane exposed to a feed containing surfactant seem denser and more compact compared to those without exposure to the surfactant.

Moreover, in case of the presence of NaCl in the feed solution, fine salt crystals of NaCl exhibit their distinctive cubic structure with significant clarity in the SEM images of the membrane surface. In fact, when the feed solution containing NaCl with higher temperatures is in contact with the membrane surface, due to the low temperature of the permeate on the other side of the membrane, the NaCl in the feed solution gets crystalized and precipitates on the surface of the membrane. To confirm the presence of existing elements on the surface of the membranes, EDX imaging was coupled with the SEM imaging, and the results are presented in Fig. 13. As expected, the results indicated that on the surface of both types of membranes (M-T and M-P), there is an amount of NaCl deposition which can lead to a potential fouling of the membrane.

Detailed compositions of the elements on the membrane surface used are presented in Table 3.

Moreover, cross-sectional SEM images of pristine and used M-T membranes employed for a feed solution containing 75 mg $\rm L^{-1}$ surfactant and 3 % NaCl at feed and permeate temperatures of 60 and 30 °C are shown in Fig. S1 to enable the active selective layer in contact with the feed solution to be seen.

4. Conclusion

The performance of a lab-pilot membrane distillation system regarding its thermal behavior and permeate flux was studied in this research. A solution of 3 % NaCl was prepared as the feed solution and after 7 h of experiment with a range of varied feed and permeate temperatures, the thermal behavior of the MD system was assessed using parameters such as GOR and SEC. The results showed that in the case of limited heat loss to the ambient, increasing feed temperatures (above 55–60 °C) along with increasing the differences between feed and permeate temperatures (typically 30–40 °C) will lead to enhanced gained output ratio (GOR) and lower specific energy consumption (SEC). These operating conditions therefore improved thermal efficiency and lowered the associated energy costs.

In the second phase, experiments with surfactant-containing feed solutions revealed important operational trade-offs. While higher feed temperatures (>60 $^{\circ}$ C) increased permeate flux, they also accelerated fouling and wetting, leading to premature termination of operation. At more moderate feed temperatures (below 55 $^{\circ}$ C), the MD process proved more stable, even with surfactant contamination, reducing the risk of fouling and maintaining flux for longer durations. Furthermore, the presence of NaCl consistently exacerbated permeate flux decline due to interactions with organic contaminants.

Although the experimental runs were limited to 25 h, the findings provide clear guidance for MD research and practice: (i) operate at moderate feed temperatures to balance flux and stability, (ii) maintain sufficient feed–permeate temperature difference to optimize energy efficiency, and (iii) consider strategies such as pretreatment to mitigate the combined effects of salts and surfactants. These insights, while based on lab-scale tests, can support the design of more energy-efficient and fouling-resistant operating strategies in industrial-scale MD systems.

CRediT authorship contribution statement

Atefeh Tizchang: Writing – review & editing, Writing – original draft, Software, Project administration, Methodology, Investigation, Formal analysis, Data curation, Conceptualization. Morgan Abily: Writing – review & editing, Supervision, Investigation, Formal analysis. Itzel Alcaraz Bernades: Methodology, Investigation. Luca Montorsi: Writing – review & editing, Funding acquisition. Hussam Jouhara: Writing – review & editing, Funding acquisition. Wolfgang Gernjak: Writing – review & editing, Validation, Supervision, Project administration, Methodology, Conceptualization.

Declaration of Competing Interest

The authors declare the following financial interests/personal relationships which may be considered as potential competing interests:

Wolfgang Gernjak reports financial support was provided by European Commission. If there are other authors, they declare that they have no known competing financial interests or personal relationships that could have appeared to influence the work reported in this paper.

Acknowledgement

The authors sincerely acknowledge the financial support from the European Union's Horizon 2020 research and innovation program for the iWAYS project (grant no 958274), as well as Departament de Recerca i Universitats de la Generalitat de Catalunya (Codi ajut: 2021 SGR 01283). Memsift Innovation Pte Ltd support during membrane distillation start-up is also appreciated.

Appendix A. Supporting information

Supplementary data associated with this article can be found in the online version at doi:10.1016/j.cherd.2025.10.025.

References

- Afsari, M., Ghorbani, A.H., Asghari, M., Shon, H.K., Tijing, L.D., 2022. Computational fluid dynamics simulation study of hypersaline water desalination via membrane distillation: effect of membrane characteristics and operational parameters. Chemosphere 305, 135294. https://doi.org/10.1016/J. CHEMOSPHERE.2022.135294.
- Akhlaghi, N., Riahi, S., 2019. Salinity effect on the surfactant critical micelle concentration through surface tension measurement. Iran. J. Oil Gas. Sci. Technol. 8, 50–63. https://doi.org/10.22050/IJOGST.2019.156537.1481.
- Ali, A., Agha Shirazi, M.M., Nthunya, L., Castro-Muñoz, R., Ismail, N., Tavajohi, N., Zaragoza, G., Quist-Jensen, C.A., 2024. Progress in module design for membrane distillation. Desalination 581, 117584. https://doi.org/10.1016/J. DESAL.2024.117584.
- Alkhudhiri, A., Darwish, N., Hilal, N., 2012. Membrane distillation: a comprehensive review. Desalination 287, 2–18. https://doi.org/10.1016/J.DESAL.2011.08.027.
- Bahmanyar, A., Asghari, M., Khoobi, N., 2012. Numerical simulation and theoretical study on simultaneously effects of operating parameters in direct contact membrane distillation. Chem. Eng. Process. Process Intensif. 61, 42–50. https://doi.org/ 10.1016/J.CEP.2012.06.012.
- Chang, J., Chang, H., Meng, Y., Zhao, H., Lu, M., Liang, Y., Yan, Z., Liang, H., 2022. Effects of surfactant types on membrane wetting and membrane hydrophobicity recovery in direct contact membrane distillation. Sep Purif. Technol. 301, 122029. https://doi.org/10.1016/J.SEPPUR.2022.122029.
- Chew, N.G.P., Zhao, S., Wang, R., 2019. Recent advances in membrane development for treating surfactant- and oil-containing feed streams via membrane distillation. Adv. Colloid Interface Sci. 273, 102022. https://doi.org/10.1016/J.CIS.2019.102022.
- Chew, N.G.P., Zhao, S., Loh, C.H., Permogorov, N., Wang, R., 2017b. Surfactant effects on water recovery from produced water via direct-contact membrane distillation. J. Memb. Sci. 528, 126–134. https://doi.org/10.1016/J.MEMSCI.2017.01.024.
- Chew, N.G.P., Zhao, S., Malde, C., Wang, R., 2017a. Superoleophobic surface modification for robust membrane distillation performance. J. Memb. Sci. 541, 162–173. https://doi.org/10.1016/J.MEMSCI.2017.06.089.
- Choudhury, M.R., Anwar, N., Jassby, D., Rahaman, M.S., 2019. Fouling and wetting in the membrane distillation driven wastewater reclamation process – a review. Adv. Colloid Interface Sci. 269, 370–399. https://doi.org/10.1016/J.CIS.2019.04.008.
- Criscuoli, A., Carnevale, M.C., 2022. Localized heating to improve the thermal efficiency of membrane distillation systems. Energies 2022 15 (15), 5990. https://doi.org/ 10.3390/EN15165990.
- Deshmukh, A., Boo, C., Karanikola, V., Lin, S., Straub, A.P., Tong, T., Warsinger, D.M., Elimelech, M., 2018. Membrane distillation at the water-energy nexus: limits, opportunities, and challenges. Energy Environ. Sci. 11, 1177–1196. https://doi.org/ 10.1039/C8EE00291F.
- Elcik, H., Fortunato, L., Alpatova, A., Soukane, S., Orfi, J., Ali, E., AlAnsary, H., Leiknes, T.O., Ghaffour, N., 2020. Multi-effect distillation brine treatment by membrane distillation: effect of antiscalant and antifoaming agents on membrane performance and scaling control. Desalination 493, 114653. https://doi.org/ 10.1016/J.DESAL.2020.114653.
- Elmarghany, M.R., El-Shazly, A.H., Salem, M.S., Sabry, M.N., Nady, N., 2019. Thermal analysis evaluation of direct contact membrane distillation system. Case Stud. Therm. Eng. 13, 100377. https://doi.org/10.1016/J.CSITE.2018.100377.
- Eykens, L., De Sitter, K., Dotremont, C., De Schepper, W., Pinoy, L., Van Der Bruggen, B., 2017. Wetting resistance of commercial membrane distillation membranes in waste streams containing surfactants and oil. Appl. Sci. 2017 7 (7), 118. https://doi.org/ 10.3390/APP7020118.
- Feng, D., Chen, Y., Wang, Z., 2023. Surfactant pretreatment as a novel fouling mitigation strategy for membrane distillation. J. Memb. Sci. 683, 121790. https://doi.org/ 10.1016/J.MEMSCI.2023.121790.
- Francis, L., Ahmed, F.E., Hilal, N., 2022. Advances in membrane distillation module configurations. Membranes 2022 12 (12), 81. https://doi.org/10.3390/ MEMBRANES12010081.

- García, J.V., Dow, N., Milne, N., Zhang, J., Naidoo, L., Gray, S., Duke, M., 2018.
 Membrane distillation trial on textile wastewater containing surfactants using hydrophobic and hydrophilic-coated Polytetrafluoroethylene (PTFE) membranes.
 Membranes 2018 8 (8), 31. https://doi.org/10.3390/MEMBRANES8020031.
- Guo, H., Gao, H., Yan, A., Lu, X., Wu, C., Gao, L., Zhang, J., 2023. Treatment to surfactant containing wastewater with membrane distillation membrane with novel sandwich structure. Sci. Total Environ. 867, 161195. https://doi.org/10.1016/J. SCITOTENV.2022.161195.
- Kalla, S., 2021. Use of membrane distillation for oily wastewater treatment a review. J. Environ. Chem. Eng. 9, 104641. https://doi.org/10.1016/J.JECE.2020.104641.
- Khayet, M., 2011. Membranes and theoretical modeling of membrane distillation: a review. Adv. Colloid Interface Sci. 164, 56–88. https://doi.org/10.1016/J. CIS.2010.09.005.
- Kronberg, B., Holmberg, K., Lindman, B., 2014. Surface chemistry of surfactants and polymers. Surf. Chem. Surfactants Polym. 1–479. https://doi.org/10.1002/ 9781118695968, 9781119961246.
- Leaper, S., Abdel-Karim, A., Gorgojo, P., 2021. The use of carbon nanomaterials in membrane distillation membranes: a review. Front. Chem. Sci. Eng. 2021 15 (4 15), 755–774. https://doi.org/10.1007/S11705-020-1993-Y.
- Lou, M., Fang, X., Huang, S., Li, J., Liu, Y., Chen, G., Li, F., 2022. Effect of cations on surfactant induced membrane wetting during membrane distillation. Desalination 532, 115739. https://doi.org/10.1016/J.DESAL.2022.115739.
- Lu, K.J., Chen, Y., Chung, T.S., 2019. Design of omniphobic interfaces for membrane distillation – a review. Water Res. 162, 64–77. https://doi.org/10.1016/J. WATRES.2019.06.056.
- Merck | Spain | Life Science Products & Service Solutions, (n.d.). (https://www.sigmaaldrich.com/ES/en) (Accessed October 17, 2024).
- Miladi, R., Frikha, N., Kheiri, A., Gabsi, S., 2019. Energetic performance analysis of seawater desalination with a solar membrane distillation. Energy Convers. Manag. 185, 143–154. https://doi.org/10.1016/J.ENCONMAN.2019.02.011.
- Miyagishi, S., Okada, K., Asakawa, T., 2001. Salt effect on critical micelle concentrations of nonionic surfactants, N-Acyl-N-methylglucamides (MEGA-n). J. Colloid Interface Sci. 238, 91–95. https://doi.org/10.1006/JCIS.2001.7503.
- Pangarkar, B.L., Deshmukh, S.K., Sapkal, V.S., Sapkal, R.S., 2016. Review of membrane distillation process for water purification. Desalin. Water Treat. 57, 2959–2981. https://doi.org/10.1080/19443994.2014.985728.
- Powdered activated carbon (PAC) vacuum-assisted air gap membrane distillation (V-AGMD) hybrid system to treat wastewater containing surfactants: Effect of operating conditions, (n.d.). (https://www.eeer.org/journal/view.php?doi=10.4491/eer.202 0.377) (Accessed September 26, 2024).
- Ramlow, H., Ferreira, R.K.M., Marangoni, C., Machado, R.A.F., 2019. Ceramic membranes applied to membrane distillation: a comprehensive review. Int. J. Appl. Ceram. Technol. 16, 2161–2172. https://doi.org/10.1111/UJAC.13301.
- Rezaei, M., Warsinger, D.M., Lienhard V, J.H., Duke, M.C., Matsuura, T., Samhaber, W. M., 2018. Wetting phenomena in membrane distillation: mechanisms, reversal, and prevention. Water Res. 139, 329–352. https://doi.org/10.1016/J. WATRES.2018.03.058.
- Shadloo, A., Peyvandi, K., Shojaeian, A., 2022. How the CMC adjust the liquid mixture density and viscosity of non-ionic surfactants at various temperatures? J. Mol. Liq. 347, 117971. https://doi.org/10.1016/J.MOLLIQ.2021.117971.
- Suárez, F., Del Río, M.B., Aravena, J.E., 2022. Water flux prediction in direct contact membrane distillation subject to inorganic fouling. Membranes 12, 157. https://doi. org/10.3390/MEMBRANES12020157/S1.
- Swaminathan, J., Chung, H.W., Warsinger, D.M., AlMarzooqi, F.A., Arafat, H.A., Lienhard, J.H., 2016b. Energy efficiency of permeate gap and novel conductive gap membrane distillation. J. Memb. Sci. 502, 171–178. https://doi.org/10.1016/J. MEMSCI.2015.12.017.
- Swaminathan, J., Chung, H.W., Warsinger, D.M., Lienhard V, J.H., 2016a. Membrane distillation model based on heat exchanger theory and configuration comparison. Appl. Energy 184, 491–505. https://doi.org/10.1016/J.APENERGY.2016.09.090.
- Swaminathan, J., Chung, H.W., Warsinger, D.M., Lienhard V, J.H., 2018. Energy efficiency of membrane distillation up to high salinity: evaluating critical system size and optimal membrane thickness. Appl. Energy 211, 715–734. https://doi.org/10.1016/J.APENERGY.2017.11.043.
- Tan, Y.Z., Velioglu, S., Han, L., Joseph, B.D., Unnithan, L.G., Chew, J.W., 2019. Effect of surfactant hydrophobicity and charge type on membrane distillation performance. J. Memb. Sci. 587, 117168. https://doi.org/10.1016/J.MEMSCI.2019.117168.
- Tijing, L.D., Woo, Y.C., Choi, J.S., Lee, S., Kim, S.H., Shon, H.K., 2015. Fouling and its control in membrane distillation—a review. J. Memb. Sci. 475, 215–244. https://doi.org/10.1016/J.MEMSCI.2014.09.042.
- Tomczak, W., Gryta, M., 2021. Membrane distillation of saline water contaminated with oil and surfactants. Membranes 2021 11 (11), 988. https://doi.org/10.3390/MEMBRANES11120988.
- Ullah, R., Khraisheh, M., Esteves, R.J., McLeskey, J.T., AlGhouti, M., Gad-el-Hak, M., Vahedi Tafreshi, H., 2018. Energy efficiency of direct contact membrane distillation. Desalination 433, 56–67. https://doi.org/10.1016/J.DESAL.2018.01.025.
- Wen, X., Li, F., Jiang, B., Zhang, X., Zhao, X., 2018. Effect of surfactants on the treatment of radioactive laundry wastewater by direct contact membrane distillation. J. Chem. Technol. Biotechnol. 93, 2252–2261. https://doi.org/10.1002/JCTB.5568.
- Yadav, A., Labhasetwar, P.K., Shahi, V.K., 2021. Membrane distillation using low-grade energy for desalination: A review. J. Environ. Chem. Eng. 9, 105818. https://doi. org/10.1016/J.JECE.2021.105818.
- Yao, M., Tijing, L.D., Naidu, G., Kim, S.H., Matsuyama, H., Fane, A.G., Shon, H.K., 2020a. A review of membrane wettability for the treatment of saline water deploying

membrane distillation. Desalination 479, 114312. https://doi.org/10.1016/J.

DESAL.2020.114312.

Yao, M., Tijing, L.D., Naidu, G., Kim, S.H., Matsuyama, H., Fane, A.G., Shon, H.K., 2020b.

A review of membrane wettability for the treatment of saline water deploying

membrane distillation. Desalination 479, 114312. https://doi.org/10.1016/J. DESAL.2020.114312.

Zhang, Y., Peng, Y., Ji, S., Li, Z., Chen, P., 2015. Review of thermal efficiency and heat recycling in membrane distillation processes. Desalination 367, 223–239. https:// doi.org/10.1016/J.DESAL.2015.04.013.